9. Principle of Optical Fibre Mode Theory

Dr. P. K. Jha

Assistant Professor,
Dept. of Physics, M. L. S. M. College, Darbhanga, Bihar.

Prof. Madan Kumar Mahto

Dept. of Physics, K. S. R. College, Sarairanjan, Samastipur.

ABSTRACT

A list of field responses for multi - mode strands allowing the registration of a modular dispersion can be compared to close field power profiles is provided in this Chapter. LP modes are categorized into bunches of mode.

The problem of keeping defective modes away from being dispatched in evaluated record strands is highlighted and the use of the mode cover essential to the efficiency of coupling within the filaments is shown.

KEYWORDS

Optical Fibre, Fiber graded index, Modes of Leaky, Integral Mode Overlap.

Step Index Fibre:

Maxwell's conditions depict electromagnetic miracles. These might be used to define the equation Wave that shows the current electric field vector E [1] generation:

$$\nabla^2 \overline{E} - \frac{\varepsilon_r}{c^2} \frac{\partial^2 \overline{E}}{\partial t^2} = 0 \qquad \textbf{(1.1)}$$

Where ∇^2 is the operator Laplacian supplied by the polar coordinates

$$\nabla^2 = \frac{\partial^2}{\partial r^2} + \frac{1}{r}\frac{\partial}{\partial r} + \frac{1}{r^2}\frac{\partial^2}{\partial \phi^2} + \frac{\partial^2}{\partial z^2} \qquad \textbf{(1.2)}$$

The term ε_r is related allow ability, while c is the vacuum light speed.

Fiber methods are wave responses that meet specified limit conditions and have a spatial appropriation that remains constant as they multiply. The fibre cladding is designed to achieve infiniteness for the sake of simplicity. This assumption is significant in view of the fact that the force in the most remarkable demand modes, in both step index and evaluated list strands with a breadth of 50um centre, falls below 10^{-22} its peak to a faultless estimate, incentive for an outspread 62.5um, the normal sweep cover for the filaments used in this project.

In polar coordinates, the results for E take the form of separability:

$E(r, \phi, z, t) = F(r)e^{j(\eta\phi)}e^{j(\beta z - \omega t)}$ **(1.3)**

Where:

aF (r) is function of the radial field,

Function periodic is an $e^{j(\eta\phi)}$,

η The number of the Azimuthal mode and the integer values are taken,

Azimuthal angleis the ϕ,

$e^{j(\beta z - \omega t)}$ is a periodic function of distance and time is $ae^{j(\beta z - \omega t)}$,

$e^{j(\beta z - \omega t)}$ is a regular distance and time function is $ae^{j(\beta z - \omega t)}$,

β Is the constant propagation & w is the optical wave's angular frequency.

Substituting eqns. (1.3) & (1.2) into eqⁿ. (1.1) gives

$$\frac{\partial^2 F}{\partial r^2} + \frac{1}{r}\frac{\partial F}{\partial r} - \frac{\eta^2}{r^2}F - \beta^2 F + \frac{\omega^2}{v^2}F = 0$$

(1.4)

Rearranging gives

$$r^2\frac{\partial^2 F}{\partial r^2} + r\frac{\partial F}{\partial r} + \left[r^2\left(n_{core}^2 k_o^2 - \beta^2\right) - \eta^2\right]F = 0$$

(1.5)

This is the Bessel equation in which ko is the space-free wave count ($2\pi/\lambda$), and n_{core} is the fibre core's refractive index. The spread constant, b, takes values in the range for a bound mode

$k_o n_{clad} \leq \beta \leq k_o n_{core}$ **(1.6)**

There is a positive solution to the shape in the core of the internal arm (1.5)

$$F(r) = J_\eta \left(r \left(n_{core}^2 k_o^2 - \beta^2 \right)^{1/2} \right)$$

(3.7)

Where J_η is the order function η. Thus, F(r) has an aperiodic core radius.

The inside term is similarly negative in the cladding, and the solution is formal

$$F(r) = K_\eta \left(r \left(\beta^2 - n_{clad}^2 k_o^2 \right)^{1/2} \right)$$

(1.8)

Where K_η is the Bessel order modified function η, alternatively, the Bessel order function is set. F(r) declines exponentially in the cladding, hence

The solution of the transverse TE & TM fibre fields component is to ignore t and z in eqn. (1.3)

$$E(r, \phi) = J_\eta \left(r \left(n_{core}^2 k_o^2 - \beta^2 \right)^{1/2} \right) \cdot e^{j(\eta\phi)}$$

(1.9)

in the core, and

$$E(r, \phi) = K_\eta \left(r \left(\beta^2 - n_{clad}^2 k_o^2 \right)^{1/2} \right) \cdot e^{j(\eta\phi)}$$

(1.10)

In the cladding.

In any case, in the forward or z route there might be a little field component to be examined if precise field arrangements are established. This section leads to two more modes, namely EH and HE, dependent on the predominance of the electric or attractive field of the z-bear. In an average interchanges fiber, nonetheless, the list distinction between the center and the cladding is tiny, prompting just looking points at the center/cladding connection. In the TE and TM crossover and some TE, TM, HE and EH groups, generator variables are virtually indistinguishable, allowing linkage to linear polarized or LP modes [2]. The LP estimate thus allow eqns to represent the fibre modes in their entirety. (1.9) and (1.10).

For the calculation of mode fields, b values must be determined. The following declaration the tangent field factor in the core interface can be matched:

$$U \frac{J_{\eta\pm1}(U)}{J_\eta(U)} = \pm W \frac{K_{\eta\pm1}(W)}{K_\eta(W)}$$

(1.11)

Where,

$$U = a\left(n_{core}^2 k_o^2 - \beta^2\right)^{1/2} \qquad (1.12)$$

And,

$$W = a\left(\beta^2 - n_{clad}^2 k_o^2\right)^{1/2} \qquad (1.13)$$

For example, in Figure 1.3 where a value of $\eta=4$has been utilized, there is a picture of terms in eqn. (1.11) with a fibre having a 50-um core diameter of 0.21NA at 850nm.

β The values necessary corresponds to the crossing points for the left side and right sides of eqn of the two sets of curves (1.11).

For this particular Azimuthal mode number there are 11 modes in this case.

Each modality, with a value of η, is shown in the radial mode value μ where $\mu=1$ is the most closely disconnected mode with a maximum value of β and $\mu=11$.

The mode has the same value as the μ bis mode.
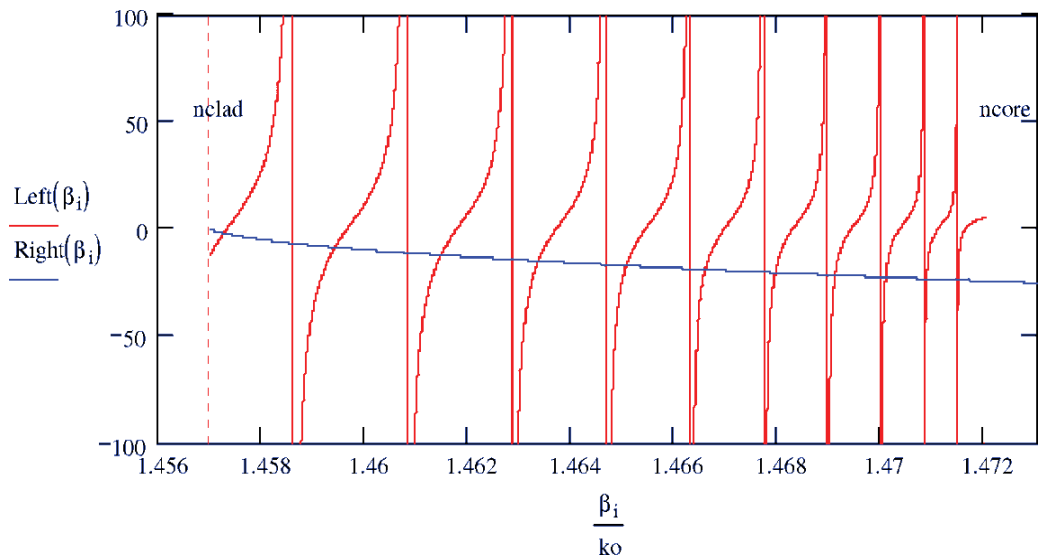
Figure 1.1: Tangent fields in the core/cladding interfaces are matched for a step index fibre to determine the spread constants
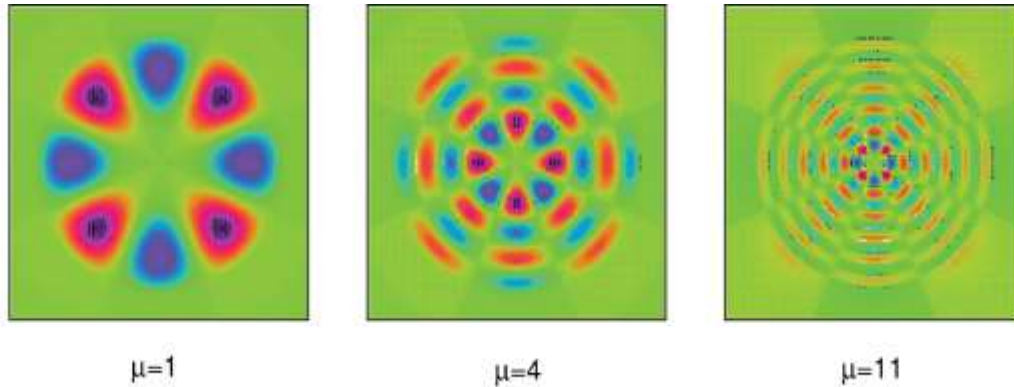
Figure 1.2: Examples of fibre-index distributions with azimuthal number of mode η=4 and varied mode numbers, μ

Then Mathcad [3] was used to calculate the fields for mode, and in Figure 1.2 some instances for η=4 are presented where the red field values are positive and the blue fields negative.

The square of the field is provided to the mode pattern which could be observed with a camera, for example. Figure 1.3 shows the respective power graphs for the above modes.
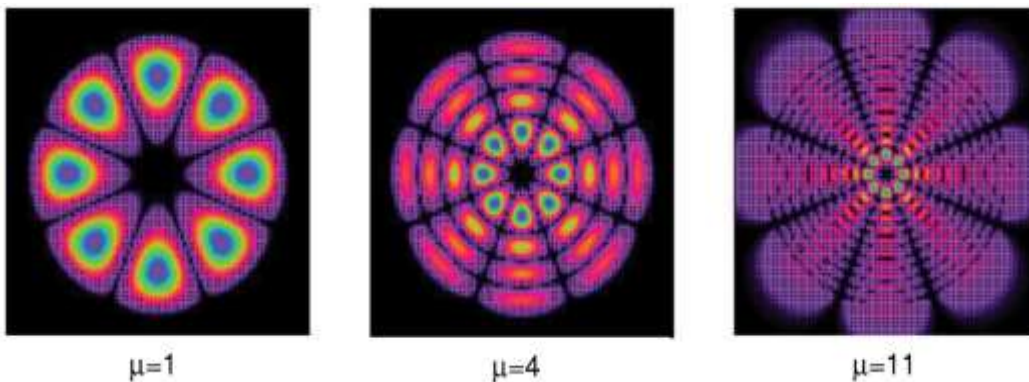
Figure 1.3: Modes with step index fibre numbers η= 4 and various mode radian numbers for the power distributions

The LP modes listed here are the conventional designations $LP_{\eta,\mu}$. M denotes the greatest number of intensities in the radial order, whereas 2η denotes the greatest number of intensities in the azimuthal direction.

(1.9) and (1.10) demonstrate that azimuthal addiction can, subject to arbitrary phase, be either $\cos(\eta\phi)$ or $\sin(\eta\phi)$.

The impact of this is to create a slightly rotated degenerate mode for two os value modes. For the two degenerated LP3, 2modes an example is provided in figure 1.4 below.

$$\mu=2,\ \eta=3$$
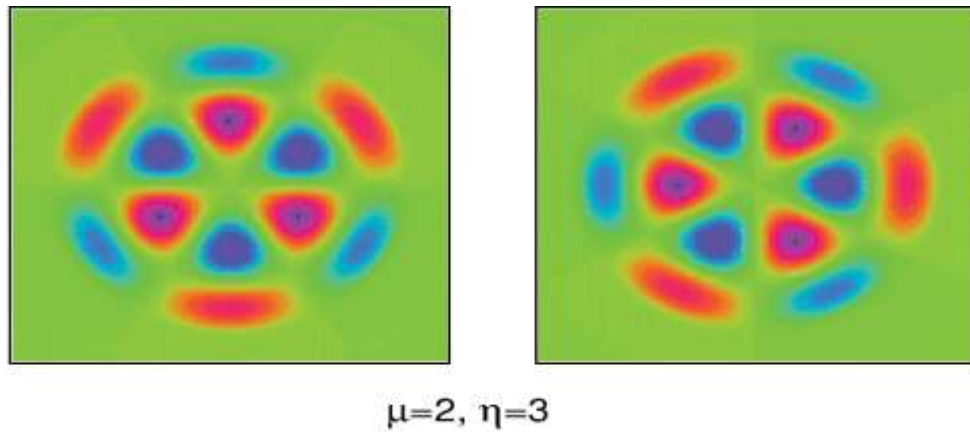
Figure 1.4: Field plots show two degenerated versions of a step-index fibre the LP$_{3,2}$ mode

Fiber Step-Index modal arousal:

A fibre step index shows about the number of modes N

$$N = \frac{V^2}{2} \tag{1.14}$$

Where the *frequency* V *normalized*, specified by:

$$V = ak_oNA \tag{1.15}$$

And the core radiusisa, the fibre numerical apertureis NA, given by,

$$NA = n_{core}\sqrt{2\Delta} \tag{1.16}$$

And the relative fibre value difference is D, as indicated by,

$$\Delta = \frac{n_{core}^2 - n_{clad}^2}{2n_{core}^2} \tag{1.17}$$

With instance, for a 50um step-index fibre, there are 753 options. This is because every LP mode, with η≠0 both orientations and two polarization states of all modes, is formed of this figure.

The force dissemination of the entire mode set was figured and immediately combined in order to generate a totally filled fibre. Figure 1.5 shows the conventional power circulation

and a profile across its centre. The power profile is usually regarded to be comparable to the progression list profile, true to shape.

(a)   (b)
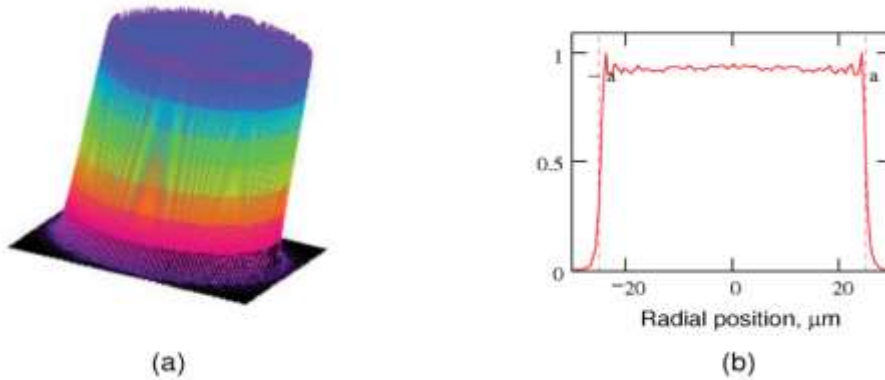
Figure 1.5: Power distribution in 50um centre diameter step-index fibre in all guided modes, equally weighted, (a) 3-D model, (b) intensity profile

Fiber Graded Index:

Take into account the power Profile n of the law index (r), supplied by,

$$n(r) = n_{core}\left[1 - 2\Delta\left(\frac{r}{a}\right)^{\alpha}\right]^{0.5} \quad \left(\frac{r}{a}\right) \leq 1$$

(1.18)

Where a factor profile is.

Allows   eqn.   (1.18)   to   replace   eqn.   (1.5),

$$r^2\frac{\partial^2 F}{\partial r^2} + r\frac{\partial F}{\partial r} + \left[r^2\left(n(r)^2 k_o^2 - \beta^2\right) - \eta^2\right]F = 0$$

(1.19)

It is the Helmholtz equation and, as is seen below with a parabolic index profile, a=2 has solutions as *Laguerre-Gauss* [4].

$$E_{\eta,\mu}(\rho, \phi, z) = \rho^{\eta} e^{\frac{-\rho^2}{2}} L_{\mu-1}^{\eta}(\rho^2) \sin(\eta\phi + \theta_o) e^{-j(\beta z)}$$

(1.20)

Where the radial variable is given by,

$$\rho = \frac{r}{a}\sqrt{V}$$

(1.21)

77

And,

$$L_{\mu'}^{\eta}(\rho^2) = \sum_{s=0}^{\mu'} \frac{(\mu'+\eta)!(-1)^s \rho^{2s}}{(\eta+s)!(\mu'-s)!s!}$$

(1.22)

Is the general polynomial of Laguerre, where the replacement $\mu'=\mu-1$ for convenience is performed.$\theta_o= 0$ or $\pi/2$, means degenerated modes pairings when THERE0.

Figure 1.6 illustrates some sample field plots for 50um, 0.21NA fibres for 850nm and distributions of the corresponding intensity in Figure 3.7.

$\mu=1, \eta=4$ $\qquad\qquad$ $\mu=4, \eta=4$
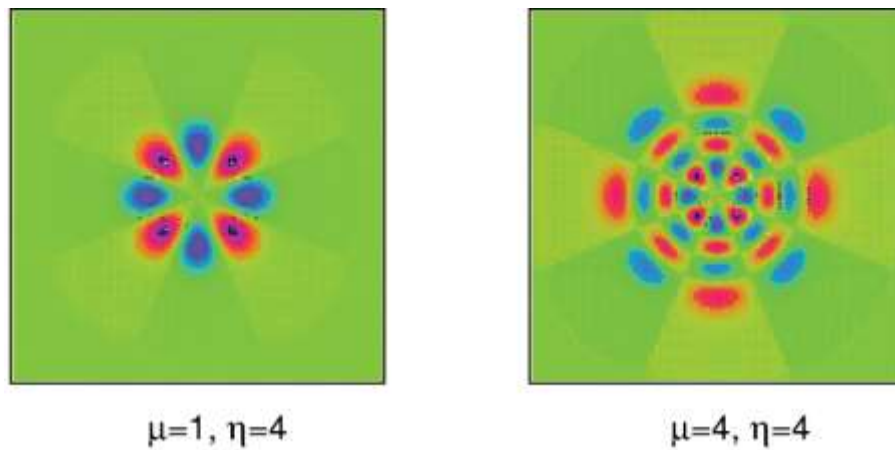
Figure 1.6: Field distribution examples for azimuth fibre mode modes with azimuth mode number η=4 and various mode numbers, μ

$\mu=1, \eta=4$ $\qquad\qquad$ $\mu=4, \eta=4$
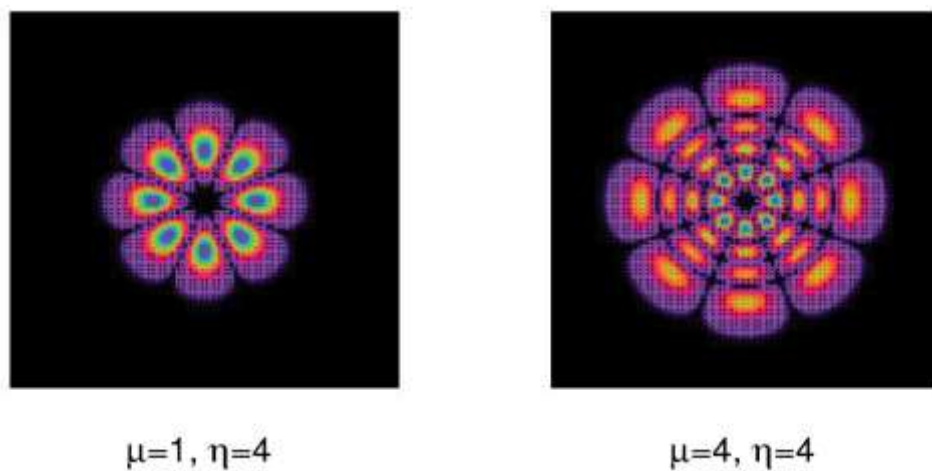
Figure 1.7: For modes in parabolic fibres with azimuthal number mode η=4 and various mode numbers, μ, power distributions examples

In comparison to Figure 1.7 with Figure 1.3, the physical size is less than the phase fibre for the same radial mode number. This can also be expressed in terms of geometric rays, where the angle of a southern ray changes constantly as the radius leaves the centre. The propagation constant is now defined as β for a specific ray,

$$\beta = k_o n (r) \cos (\theta) \qquad \textbf{(1.23)}$$

Is unchanged. Thus, in a zone with a lower reflector index of eq[n] (3, 23), the è è value is lowered and the central area is returned. Therefore, the higher order mode occupies the core diameter more than physically the lower order form.

1. Fiber graded index modal arousal:

Approximately the number of modes N in index fibre.

$$N = V^2 \left[\frac{\alpha}{2(\alpha + 2)} \right] \qquad \textbf{(1.24)}$$

For example, there are approximately 276 modes in a 50mm graded index fibre, 0,21NA at 850nm.

The linear combination of the whole parabolic index fibre mode is presented in Figure 1.8. The intensity profile of the parabolic index profile is similar.

(a)   (b)
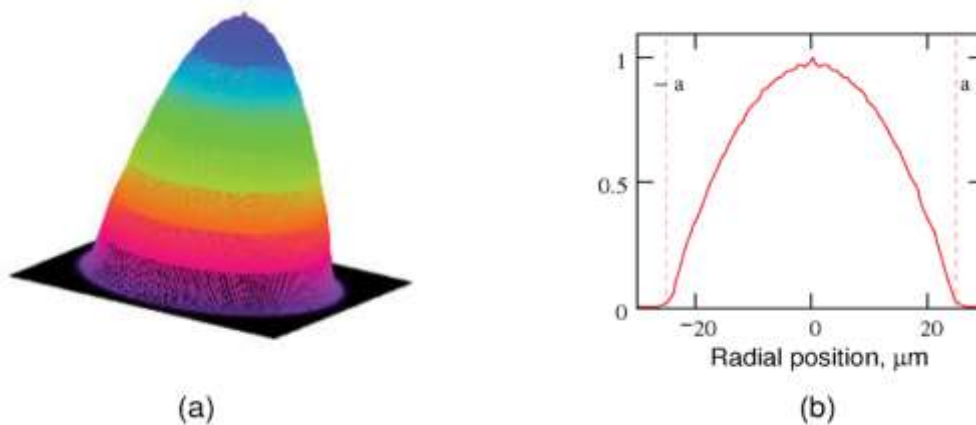
Figure 1.8: Power distribution of the parabolic index fibre 50um diameter of every conceivable guided modes, equally weighted, (a) 3-D model, (b) intensity profile

2. Groups of Mode:

The WKB approach [5] is shown in a graduation index for the mode's propagating constant [6].

$$\beta = k_o n_{core}\left(1 - 2\Delta\left(\frac{m}{M}\right)^{2\alpha_i/(2+\alpha)}\right)^{1/2}$$

(1.25)

$$m = 2\mu + \eta - 1$$

(1.26)

And the maximum number of main mode is M as shown,

$$M = \sqrt{\frac{\alpha}{\alpha + 2}} k_o n_{core} a \sqrt{\Delta}$$

(1.27)

There are numerous combinations of (η, μ) from eqn. (1.26) which have and degenerate with the same main mode number. For instance, there are 19 mode groups at 850nm from the equinox (3.27) on a parabola index fibre, with 50um core diameter and 0, 21 NA.

However, it is noteworthy that Finite Elements [8] approaches reveal that modes Often differs by around 0, 0007 in the same mode group. Percent in propagation constant. This is significantly less than the difference between neighbouring mode classes in the propagation constant, generally 0.055%.

The number of the different modes is double that of the group mode number in each mode group. Now that the modes $\eta \neq 0$ and two polarizations' states exist in each mode, as mentioned in section 3.1.1, a total of ten modes are included in that group. Figure 1.9 shows the $LP_{\eta,\mu}$ modes of the first 16 modes of fibre graded with a core diameter of 50um, at 850nm.

1	2	3	4	5	6	7	8	9	10	11	12	13	14	15	16
0 1	1 1	2 1	3 1	4 1	5 1	6 1	7 1	8 1	9 1	10 1	11 1	12 1	13 1	14 1	15 1
	0 2	1 2	2 2	3 2	4 2	5 2	6 2	7 2	8 2	9 2	10 2	11 2	12 2	13 2	
				0 3	1 3	2 3	3 3	4 3	5 3	6 3	7 3	8 3	9 3	10 3	11 3
						0 4	1 4	2 4	3 4	4 4	5 4	6 4	7 4	8 4	9 4
								0 5	1 5	2 5	3 5	4 5	5 5	6 5	7 5
										0 6	1 6	2 6	3 6	4 6	5 6
												0 7	1 7	2 7	3 7
														0 8	1 8

Figure 1.9: The first 16 fibre graded index mode classes at 850 nm. Are tabulated. Blue and LP_{η}, μ mode group numbers, green indication

If the distribution of field intensity is excited equally by all modes Pg will be displayed for each group m modes.

$$P_g(m) = \sum_{\mu=1}^{\text{int}[(m+1)/2]} \left[\left(E_{\eta,\mu}\right)^2_{\theta_o=0} + \left(E_{\eta,\mu}\right)^2_{\theta_o=\pi/2} \right]$$

(1.28)

Where, from eq^n. (1.26), $\eta=m+1-2\mu$.

The total P_{tot} distribution is determined close to the field

$$P_{tot} = \sum_{m=1}^{M} \left[P_g(m) \cdot MTF(m) \right]$$

(1.29)

Where, MTF (m)=1 for all mode values for a full-filled fibre.

Figure 1.10 shows examples of mode group 4 and 14 near field profile, in which the power distributions consist of circularly symmetric rings with rings corresponding to half mode group number. Figure 1.10 shows the power distributions.

mode group 4   mode group 14
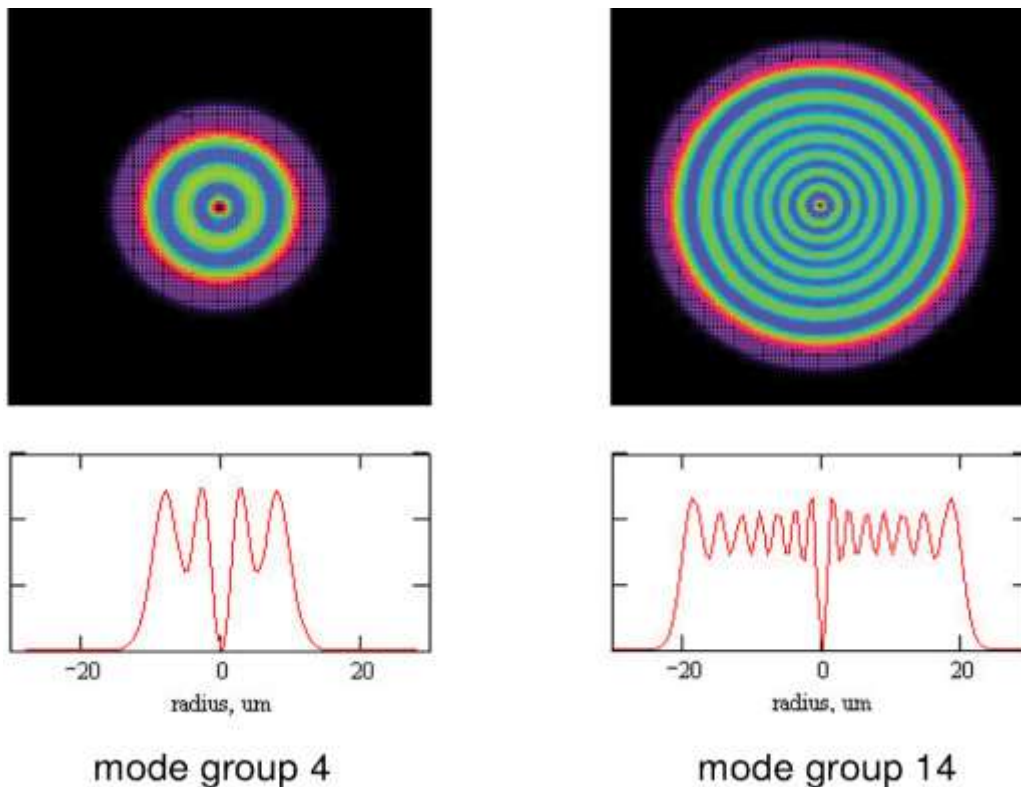
Figure 1.10: The modes 4 and 10 are intensively distributed in 50um index fibres

3. Modes of Leaky:

In the mode of guidance.

$$k_o n_{clad} \leq \beta \leq k_o n_{core} \qquad (1.30)$$

There are modes within two caustic factors inside the Helmholtz equation, eqn (3.19), defining positive coefficient values of F (r).

$$\left(n(r)^2 k_o^2 - \beta^2\right) - \left(\frac{\eta^2}{r^2}\right) \geq 0 \qquad (1.31)$$

However, there is an area in which mode is outside of the limits, but the same inequality is satisfied [7]:

$$k_o^2 n_{clad}^2 - \frac{\eta^2}{a^2} \leq \beta^2 < k_o^2 n_{clad}^2 \qquad (1.32)$$

For example, Figure 1.11, in which mode $LP_{16, 3}$ is limited to 11um through 24um and beyond 32um is radiative. Guided light can be viewed from a quantum-mechanical point of view as a tunnel in the material section through the evanescent tail in a radiation mode. Several leaky modes will be immediately attenuated after some centimeters, while others will stretch for one kilometer or more [8].
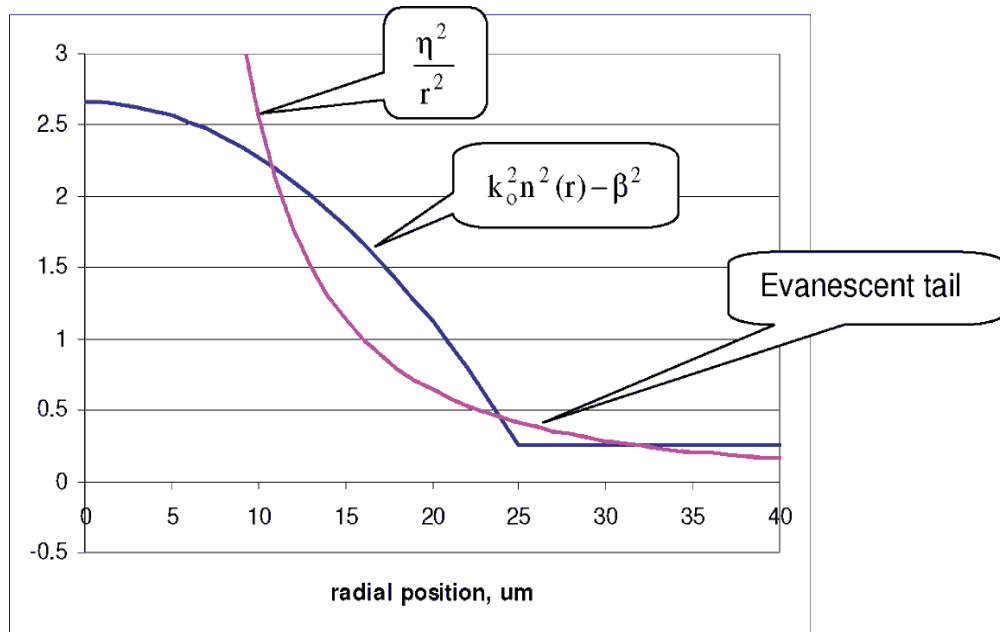
Figure 1.11: Plot of terms in leaky mode (LP16, 3), eqn (3.31)

The total number of leaky fibre modes is defined by,

$$N_{leaky} = \frac{V^2}{12}$$

(1.33)

Where:

$$V = k_o aNA$$

(1.34)

Leak mode may reach up to 25% of the overall power in a graduated index fibre in comparison to eqn (1.24).

Eqn is also used to determine the distributions of leaked modes in the field. (3.20) for the values of leaky mode [8],

$$M \leq 2\mu + \eta - 1 \leq M + \frac{\eta^2}{4M}$$

(1.35)

Where M is the eqn-mode group number (1.27),

As an example, 120 leak modes with both polarizations and orientations are found in a 50um fibre at 850nm, representing a total of 30 discreets (η, μ) combinations.

The impact of broken modes is to pull the near-field force towards dispersion. Blue added for the guided mode in Figure 1.12 was the whole defective mode range.

All guided modes have a strength profile that is considerably squareer than half of the depicted condition.

For some time now, a cracked file profiling system was a problem depending on the rule that the file profile condition will be approximately linked to the present profile if all guided modes are evenly powered.

The appearance of cracked modes actually disturbs and makes a few efforts towards rectifying the exactness of these strategies [9].

Crushed modes are difficult to keep a strategic distance because they are completely within the southern NA of a fibre.

Partially 6 will study the influence of fractured modes in control mode devices.
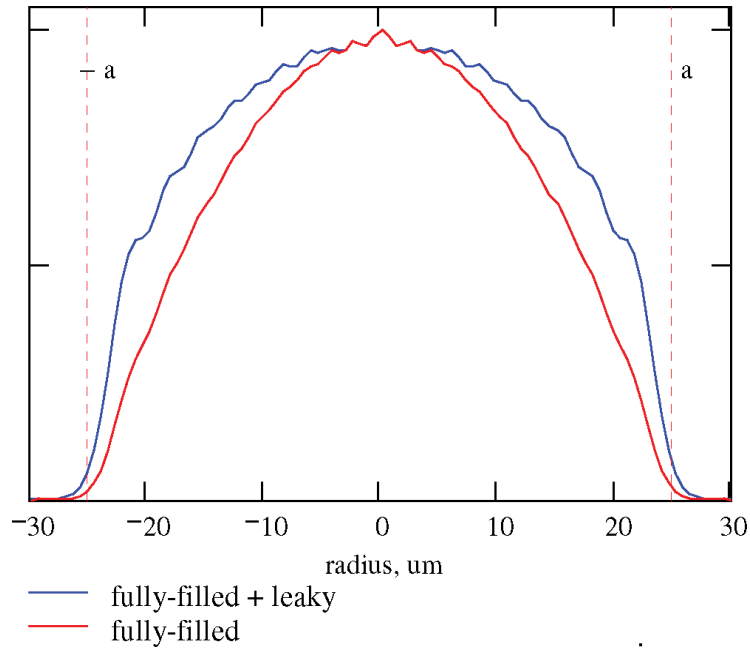
Figure 1.12: 50m graded index fibre computed near-field intensity profile with guiding modes (rot) and Difficult modes for guided modes (blue)

Integral Mode Overlap:

Factor overlap for each source mode Factor to identify a fibre mode distribution associated with the target fibre, E_S should be calculated for each target E_T mode. This calls for an integral overlap: The next item:

$$\varepsilon = \frac{\int\int E_S(x, y)E_T(x, y)dxdy}{\sqrt{\int\int E_S(x, y)E_S(x, y)dxdy}\sqrt{\int\int E_T(x, y)E_T(x, y)dxdy}}$$

(1.36)

For example, in the event of a non-overlap, which is in the same waveguide, the mode overlap might take zero to unit values for total overlap.

The overlap integral for each mode combination needs to be numerically analysed and hence intensively calculated. However, it has been discovered that modes e was insignificantly tiny in Bessel and Laguerre-Gauss (LG) for the connection between modes with a distinct azimuthal number η. Therefore, e for modes with the same value of daily use was only essential.

In Table 1.1 for example the value of a connection between $LP_{2,1}$ Bessel & $LP_{2,\mu}$ LG modes is shown by $|\varepsilon|$value. For example. Please note that the table squares are almost one, which indicates that energy is very low when combined with modes having a different azimuth mode.

Table 1.1: Laguerre-Gaussian core overlap with LP2, 1 and LP2, μ

$LP_{2,1}$	$LP_{2,2}$	$LP_{2,3}$	$LP_{2,4}$	$LP_{2,5}$	$LP_{2,6}$	$LP_{2,7}$	$LP_{2,8}$	$LP_{2,9}$
0.305	0.414	0.451	0.437	0.389	0.319	0.238	0.154	0.077

In proportion to the value sq. of their corresponding overlap coefficients, the distribution of power from the mode supplied in table 1.1 were added to the power distribution of the near field combined with the LP2, 1 mode graded fibre in the example above.

Figure 1.13 shows an LP2, 1 Bessel mode power attribution with its resulting fibre grade index power attribution.

The LP2, 1, however, power dispersed across a number of radial mode μ numbers is shown to be the same four-lobed mode.

LP$_{2,1}$ Bessel mode   Laguerre-Gauss modes
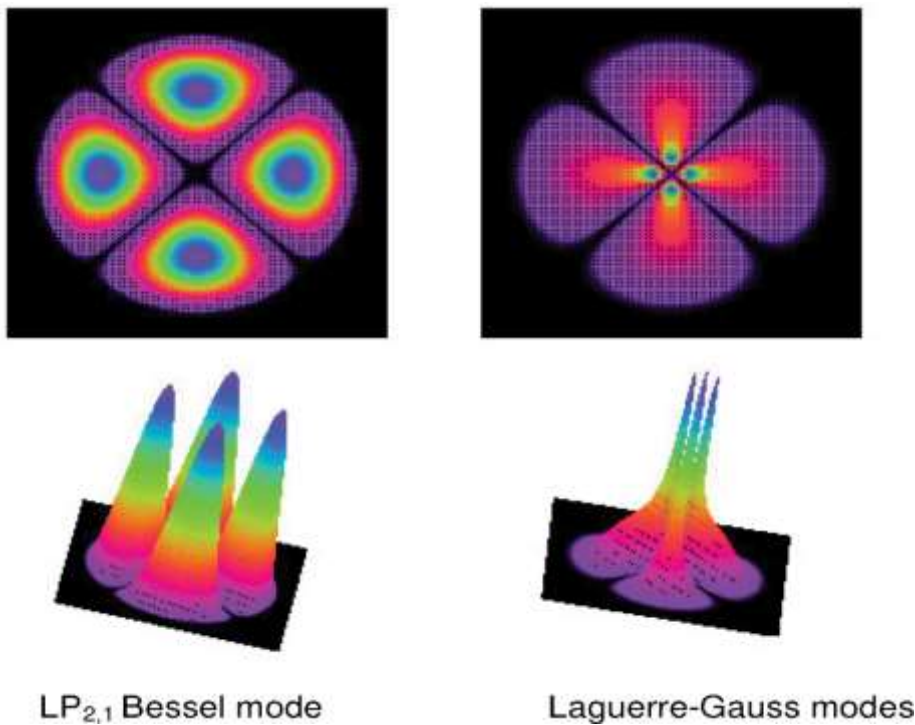
Figure 1.13: The mode power distributions in step-index fibre for the LP2, 1 Bessel fibre with index ratings mode and power distribution fibre

Discussion:

This chapter shows how to record the dispersion of mode power in the sync and illustrated record strings for each mode. The full broken mode set of a re-examined record fibre has been shown to fit within the southern mathematical gap of the assessed fibre and fractured modes may cause the force profile to bend.

References:

1. J. M. Senior, "Optical Fibre Communications", section 2.3, Prentice Hall, second edition, 1992.
2. D. Gloge, 'Weakly Guiding Fibres', Appl. Opt., vol. 10, no. 10, pp. 2252-2258, 1971. http://www.mathsoft.com
3. S. Berdague and P. Facq, 'Mode division multiplexing in optical fibres', Appl. Opt., vol. 21, no. 11, pp. 1950-1955, 1982.
4. D. Gloge and E. A. J. Marcatili, 'Impulse response of fibres with ring-shaped parabolic index distribution', Bell Syst. Tech. J., vol. 52, no. 7, pp. 1161-1168, 1973.
5. D. Gloge and E. A. J. Marcatili, 'Multimode theory of graded-core fibres', Bell Syst. Tech. J., vol. 52, no. 9, pp. 1563-1579, 1973.
6. Y. Liu et al., 'Accurate mode characterization of the graded-index multimode fibres for the application of mode-noise analysis', Appl. Opt., vol. 34, no. 9, pp. 1540-1543, 1995.
7. M. J. Adams et al., 'Leaky rays on optical fibres of arbitrary (circularly symmetric) index profiles', Electron. Lett., vol. 11, no. 11, pp. 238-240, 1975.
8. R. Olshansky, 'Leaky modes in graded index optical fibres', Appl. Opt., vol. 15, no. 11, pp. 2773-2777, 1976.
9. F. Sladen et al., 'Determination of optical fibre refractive index profiles by a near-field scanning technique', Appl. Phys. Lett., vol. 28, no. 8, pp. 225-258, 1976.